Kazimierz MIKOŁAJUK, Andrzej TOBOŁA

Warsaw University of Technology

Ripple Analysis for Three-Phase Four-Leg Active Power Filters

Abstract. *The paper presents the analytical method of ripple estimation in active power filters. The method is based on an average model of PWM voltage source inverter. The formulae for the ripple magnitude are derived for three-phase four-leg structures. The numerical example for filters generating third order harmonics is presented.*

Streszczenie. *Przedstawiono analityczną metodę estymacji tętnienia prądu wynikającego z przełączeń obwodu w aktywnych filtrach energetycznych. Metoda opiera się na uśrednionych modelach z modulacją PWM. Odpowiednie formuły analityczne zostały opracowane dla układu trójfazowego czteroprzewodowego. Wykonano obliczenia dla układu generującego trzecią harmoniczną prądu.* ***(Analiza tętnień prądu w trójfazowych czteroprzewodowych strukturach aktywnych filtrów energetycznych).***

Keywords: averaging techniques for switching circuits, current ripple, active power filters.
Słowa kluczowe: metoda uśredniania układów przełączanych, tętnienia prądu, aktywne filtry energetyczne.

Introduction

The wide use of consumer electronics and power electronic based products in industries causes current and voltage pollution in power distribution system. Active power filters have been developed to clean harmonics from power supply. The main components of active power filters are voltage source inverters.

An important feature of power electronic circuits working in switching scheme is a ripple effect. Switching frequency errors are undesirable effects always accompanying these techniques [1]. The magnitude of current ripples can be computed by simulation of a specific PWM realisation. More general information can be obtained from analytical formulae. Such formulae can be derived when an average model of PWM inverter is employed. Average models simplify analysis and speed up simulation. The analytical method of ripple estimation in single-phase and three-phase three-wire structures of active power filters is presented in [3]. To compensate the harmonic current through the neutral point the four-wire structure of active power filter is needed. The presented paper provides the method of ripple analysis in three-phase four-leg active power filters.

Three-dimensional space vector modulation

Three-phase voltage source inverters normally have two ways of improving a neutral connection for three-phase four-wire systems: using split dc link capacitors and using a four-leg inverter topology. From comparative study it is found that the three-phase four-leg topology is best suited for unbalanced and nonlinear load compensation in three-phase four-wire systems [2]. This topology is illustrated in Fig. 1. The active power filter (Fig. 1) consists of voltage source inverter with power switches and anti-parallel diodes, dc capacitor and interface inductors. A properly switched circuit should generate such phase currents that are as close to reference signal as possible. The switching combinations can be represented by the ordered sets of four letters *p* and *n*, where *p* denotes that the upper switch in phase line 'a,b,c' or 'N' is closed and *n* denotes that this switch is opened. For example the set (*pnnn*) denotes that upper switch in line 'a' is closed and all remained upper switches are opened. The switch state at time instant *t* can be bound with phase switching function $S_{ph}(t) = [s_a(t) \quad s_b(t) \quad s_c(t)]^T$. The entries of matrix $S_{ph}(t)$ can be equal 1, 0 or -1. This switching function shows how the dc voltage V_C is inserted to the individual phase line.

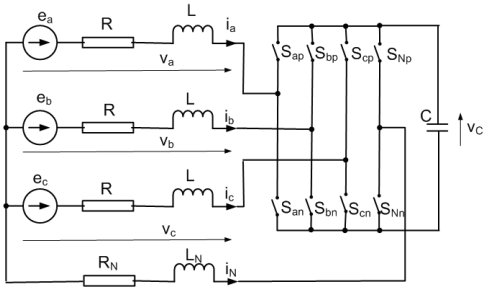

Fig. 1. Three-phase four-leg active filter

The total number of switching combinations in four-leg inverters is sixteen [2]. Table 1 shows switching function S_{ph} for all sixteen switching combinations.

Table 1. Mapping of switching combination into switching matrix S_{ph}

pppp	*nnnp*	*pnnp*	*ppnp*	*npnp*	*nppp*	*nnpp*	*pnpp*
$\begin{bmatrix}0\\0\\0\end{bmatrix}$	$\begin{bmatrix}-1\\-1\\-1\end{bmatrix}$	$\begin{bmatrix}0\\-1\\-1\end{bmatrix}$	$\begin{bmatrix}0\\0\\-1\end{bmatrix}$	$\begin{bmatrix}-1\\0\\-1\end{bmatrix}$	$\begin{bmatrix}-1\\0\\0\end{bmatrix}$	$\begin{bmatrix}-1\\-1\\0\end{bmatrix}$	$\begin{bmatrix}0\\-1\\0\end{bmatrix}$
pppn	*nnnn*	*pnnn*	*ppnn*	*npnn*	*nppn*	*nnpn*	*pnpn*
$\begin{bmatrix}1\\1\\1\end{bmatrix}$	$\begin{bmatrix}0\\0\\0\end{bmatrix}$	$\begin{bmatrix}1\\0\\0\end{bmatrix}$	$\begin{bmatrix}1\\1\\0\end{bmatrix}$	$\begin{bmatrix}0\\1\\0\end{bmatrix}$	$\begin{bmatrix}0\\1\\1\end{bmatrix}$	$\begin{bmatrix}0\\0\\1\end{bmatrix}$	$\begin{bmatrix}1\\0\\1\end{bmatrix}$

For given capacitor voltage V_C the state equation of the circuit shown in Fig. 1 can be written as

$$\begin{bmatrix}e_a\\e_b\\e_c\end{bmatrix} - \begin{bmatrix}L+L_N & L & L\\ L & L+L_N & L\\ L & L & L+L_N\end{bmatrix}\frac{d}{dt}\begin{bmatrix}i_a\\i_b\\i_c\end{bmatrix} - \begin{bmatrix}R+R_N & R & R\\ R & R+R_N & R\\ R & R & R+R_N\end{bmatrix}\begin{bmatrix}i_a\\i_b\\i_c\end{bmatrix} = S_{ph}(t)V_C \tag{1}$$

The orthogonal coordinate transformation should be applied. Transformation matrices T and T^{-1} are expressed as

(2) $$T=\frac{1}{3}\begin{bmatrix}1 & 1 & 1\\ 2 & -1 & -1\\ 0 & \sqrt{3} & -\sqrt{3}\end{bmatrix}$$

(3) $$T^{-1}=\begin{bmatrix}1 & 1 & 0\\ 1 & -\frac{1}{2} & \frac{\sqrt{3}}{2}\\ 1 & -\frac{1}{2} & -\frac{\sqrt{3}}{2}\end{bmatrix}$$

After multiplying both sides of (1) with matrix T three independent equations for 0, α and β components are obtained

(4) $\upsilon_0 = s_0(t)V_C \qquad \upsilon_\alpha = s_\alpha(t)V_C \qquad \upsilon_\beta = s_\beta(t)V_C$

where

(5) $$\upsilon_0 = e_0 - (L+3L_N)\frac{di_0}{dt} - (R+3R_N)i_0$$

(6) $$\upsilon_\alpha = e_\alpha - L\frac{di_\alpha}{dt} - Ri_\alpha$$

(7) $$\upsilon_\beta = e_\beta - L\frac{di_\beta}{dt} - Ri_\beta$$

and orthogonal switching function

(8) $$S(t)=\begin{bmatrix}s_0(t)\\ s_\alpha(t)\\ s_\beta(t)\end{bmatrix}=TS_{ph}(t)$$

The orthogonal switching matrix for all switch combination is presented in Table 2.

In three dimensional space the vectors $V_C S$ can be illustrated as shown in Fig. 2a. There are two zero switching vectors *pppp, nnnn* and fourteen nonzero vectors [2]. Projection of the sixteen switching vectors on the α-β plane forms the hexagon shown in Fig. 2b.

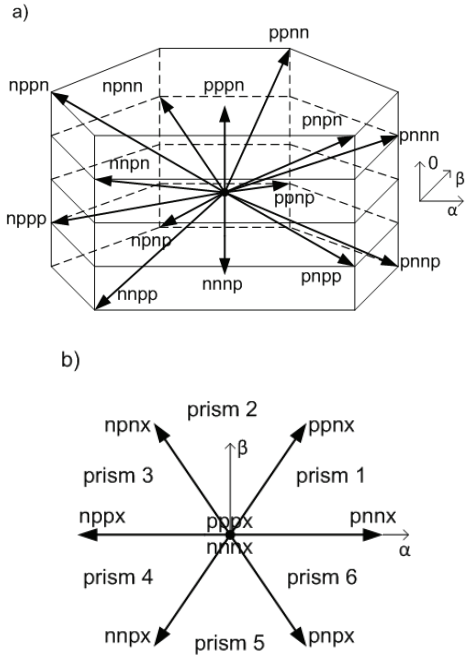

Fig. 2. Switching vectors in 0-α-β coordinates

For switching instant $t = t_k$ the reference vector

(9) $$\upsilon_{ref}(t_k) = \left[\upsilon_{ref0}(t_k) \quad \upsilon_{ref\alpha}(t_k) \quad \upsilon_{ref\beta}(t_k)\right]^T$$

with matrix entries defined by (5)-(7) is synthesized within switching interval $(t_k, t_k + T_s)$, using three nonzero vectors shown in Fig. 2a and one zero vector. Within switching period T_s each of four vectors are on duty during the proper intervals d_1T_s, d_2T_s, d_3T_s and $(1-d_1-d_1-d_3)T_s$, where d_1, d_2 and d_3 are duty ratios.

The synthesis of the reference vector means selection of three nonzero switching vectors and one zero vector, and then computation of duty ratios corresponding to chosen vectors [2]. Each of three chosen nonzero vectors is equivalent to switching function $S(t)$ defined in (8).

The selection of three nonzero vectors takes two steps: prism identification and tetrahedron identification.

The prism identification is based on the projection of reference vector υ_{ref} on the α-β plane (Fig. 2b). There are six prisms associated with six 60° sectors on the α-β plane.

Table 2. Mapping of switching combination into switching matrix S

pppp	*nnnp*	*pnnp*	*ppnp*	*npnp*	*nppp*
$\begin{bmatrix}0\\0\\0\end{bmatrix}$	$\begin{bmatrix}-1\\0\\0\end{bmatrix}$	$\begin{bmatrix}-\frac{2}{3}\\ \frac{2}{3}\\ 0\end{bmatrix}$	$\begin{bmatrix}-\frac{1}{3}\\ \frac{1}{3}\\ \frac{1}{\sqrt{3}}\end{bmatrix}$	$\begin{bmatrix}-\frac{2}{3}\\ \frac{1}{\sqrt{3}}\\ \frac{1}{\sqrt{3}}\end{bmatrix}$	$\begin{bmatrix}-\frac{1}{3}\\ -\frac{2}{3}\\ 0\end{bmatrix}$
nnpp	*pnpp*	*pppn*	*nnnn*	*pnnn*	*ppnn*
$\begin{bmatrix}-\frac{2}{3}\\ -\frac{1}{3}\\ -\frac{1}{\sqrt{3}}\end{bmatrix}$	$\begin{bmatrix}-\frac{1}{3}\\ \frac{1}{3}\\ -\frac{1}{\sqrt{3}}\end{bmatrix}$	$\begin{bmatrix}1\\0\\0\end{bmatrix}$	$\begin{bmatrix}0\\0\\0\end{bmatrix}$	$\begin{bmatrix}\frac{1}{3}\\ \frac{2}{3}\\ 0\end{bmatrix}$	$\begin{bmatrix}\frac{2}{3}\\ \frac{1}{3}\\ \frac{1}{\sqrt{3}}\end{bmatrix}$
npnn	*nppn*	*nnpn*	*pnpn*		
$\begin{bmatrix}\frac{1}{3}\\ -\frac{1}{3}\\ \frac{1}{\sqrt{3}}\end{bmatrix}$	$\begin{bmatrix}\frac{2}{3}\\ -\frac{2}{3}\\ 0\end{bmatrix}$	$\begin{bmatrix}\frac{1}{3}\\ -\frac{1}{3}\\ -\frac{1}{\sqrt{3}}\end{bmatrix}$	$\begin{bmatrix}\frac{2}{3}\\ \frac{1}{3}\\ -\frac{1}{\sqrt{3}}\end{bmatrix}$		

For example, the first prism associated with the first sector $0-60^\circ$ is shown in Fig. 3a.

Within the selected prism, there are six nonzero zero vectors and two zero vectors. Four tetrahedrons can be stretched on each vector triple chosen from six vectors placed in selected prism. These tetrahedrons are numbered from 1 to 4. For example, the tetrahedron 1st in the prism 1st is shown in Fig. 3b.

The criterion of tetrahedron choice, when prism is selected is based on phase voltage polarities in *a-b-c* coordinates [2]. The voltage polarities of the reference vector elements are compared with those of the vectors of each tetrahedron. It means that the polarities of the chosen switching function $S(t)$ cannot be opposite to the polarities of the reference vector υ_{ref}. For example, let us assume that the reference voltage is located in prism 1 and phase

voltage polarities are $\upsilon_{refa} > 0, \upsilon_{refb} < 0, \upsilon_{refc} < 0$. The tetrahedron shown in Fig. 3b should be chosen, since the vectors of this tetrahedron has the polarities +00, 0- -, 00- and they are not opposite to the phase voltage polarities + - - . Within each tetrahedron all vectors produce nonconflicting line to neutral voltages, thus they are adjacent vectors. Such control minimize the circulating energy [2].

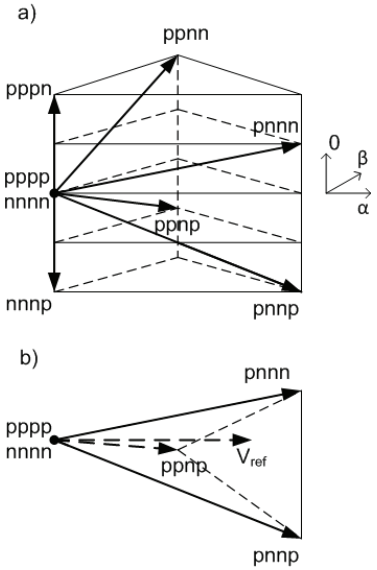

Fig. 3. The first prism and first tetrahedron in this prism

Average functions and ripple functions

The averaging operator within the moving interval $(t - T_S, t)$

$$\xi_{av} = \frac{1}{T_S}\int_{t-T_S}^{t} \xi(\tau) d\tau \tag{10}$$

can be applied to state equations (4)-(8).
Switching period T_S is small in comparison with the periods of the harmonics to be generated by active filters. It means that variations of state variables $i(t)$ and $\upsilon_C(t)$ within interval $(t - T_S, t)$ is small and the following approximation is acceptable

$$\frac{1}{T_S}\int_{t-T_S}^{t} s(\tau)x(\tau)d\tau = s_{av}(t)x_{av}(t) \tag{11}$$

where $x(t)$ state variable, $s(t)$ discontinuous switching function, $x_{av}(t)$ average state variable and $s_{av}(t)$ average switching function.
Applying the averaging operator (10) to equations (3)-(6) and taking in account approximation (11), we obtain

$$\upsilon_{av} = V_C S_{av} \tag{12}$$

where average matrices are

$$\upsilon_{av} = \begin{bmatrix} \upsilon_{av0} \\ \upsilon_{av\alpha} \\ \upsilon_{av\beta} \end{bmatrix} \quad S_{av} = \begin{bmatrix} s_{av0} \\ s_{av\alpha} \\ s_{av\beta} \end{bmatrix} \tag{13}$$

Let us consider chosen switching period T_S and corresponding to this period the selected tetrahedron with three nonzero vectors $V_C S_1$, $V_C S_2$, $V_C S_3$ and one zero vector. The average switching matrix S_{av} is the result of the application of operator (10) to the sequence of the four vectors and corresponding to them switching matrices shown in Table 2. The entries s_{av0}, $s_{av\alpha}$, $s_{av\beta}$ of the S_{av} are the result of the averaging of the discontinuous switching functions $s_0(t)$, $s_\alpha(t)$, and $s_\beta(t)$. Within the selected period T_S, during intervals $d_1 T_S$, $d_2 T_S$ and $d_3 T_S$ functions remain constant and equal to the sequence of three switching matrices placed in Table 2 and corresponding to the selected tetrahedron. Within the interval $(1 - d_1 - d_1 - d_3)T_S$ the zero vector is on duty. It means that

$$S_{av} = \begin{bmatrix} S_1 & S_2 & S_3 \end{bmatrix} \begin{bmatrix} d_1 \\ d_2 \\ d_3 \end{bmatrix} \tag{14}$$

On the other hand the average voltage υ_{av} on the left side of (12) should be equal to reference voltage υ_{ref} given in (9), hence

$$S_{av} = \frac{1}{V_C}\upsilon_{ref} \tag{15}$$

and taking into account (14), we obtain duty ratios

$$\begin{bmatrix} d_1 \\ d_2 \\ d_3 \end{bmatrix} = \frac{1}{V_C}\begin{bmatrix} S_1 & S_2 & S_3 \end{bmatrix}^{-1} \begin{bmatrix} \upsilon_{ref0} \\ \upsilon_{ref\alpha} \\ \upsilon_{ref\beta} \end{bmatrix} \tag{16}$$

For example, if for interval $(t_k, t_k + T_S)$ the reference voltage $\upsilon_{ref}(t_k)$ is given and placed within the selected tetrahedron shown in Fig. 3b with vectors *pnnn, pnnp* and *ppnp* , then according to Table 2

$$\begin{bmatrix} d_1 \\ d_2 \\ d_3 \end{bmatrix} = \frac{1}{V_C}\begin{bmatrix} \frac{2}{3} & \frac{2}{3} & \frac{1}{3} \\ 0 & 0 & \frac{1}{\sqrt{3}} \\ \frac{1}{3} & -\frac{2}{3} & -\frac{1}{3} \end{bmatrix}^{-1} \begin{bmatrix} \upsilon_{ref0} \\ \upsilon_{ref\alpha} \\ \upsilon_{ref\beta} \end{bmatrix} \tag{17}$$

The capacitor voltage V_C is the average voltage within considered interval $(t_k, t_k + T_S)$ and it depends on t_k.

The method of ripple estimation for three-phase four-leg voltage source converter can be developed from the method presented in [3] for the single-phase and three-phase three-leg circuits.

Let us consider equations (4)-(7) for $t \in (t_k, t_k + T_S)$ under the following assumptions: $e_0(t) = e_{av0}(t_k)$, $e_\alpha(t) = e_{av\alpha}(t_k)$, $e_\beta(t) = e_{av\beta}(t_k)$, $s_0(t) = s_{av0}(t_k)$, $s_\alpha(t) = s_{av\alpha}(t_k)$, $s_\beta(t) = s_{av\beta}(t_k)$, $V_C(t) = V_C(t_k)$ and $R = R_N = 0$. For such assumptions currents $i_{av0}(t)$, $i_{av\alpha}(t)$, $i_{av\beta}(t)$ obtained as solutions of equations (4)-(7) are

$$i_{av0}(t) = i_{av0}(t_k) + \frac{e_{av0}(t_k) - s_{av0}(t_k)V_C(t_k)}{L + 3L_N}(t - t_k) \tag{18}$$

$$i_{av\alpha}(t) = i_{av\alpha}(t_k) + \frac{e_{av0}(t_k) - s_{av\alpha}(t_k)V_C(t_k)}{L}(t - t_k) \tag{19}$$

$$i_{av\beta}(t) = i_{av\beta}(t_k) + \frac{e_{av\beta}(t_k) - s_{av\beta}(t_k)V_C(t_k)}{L}(t - t_k) \tag{20}$$

The approximated piecewise linear waveforms of averaged current $i_{av}(t)$ and actual rippled current $i(t)$ within single switching period T_s are shown in Fig.4. The segment AE in Fig. 4 illustrates equations (18)-(20).

The deviation level of real generated current waveform from the smooth average waveform is the result of discontinuity of switching functions. For interval $(t_k, t_k + d_1 T_s)$ the actual currents can be expressed as follows

$$i_0(t) = i_0(t_k) + \frac{e_{av0}(t_k) - s_{10}(t_k) V_C(t_k)}{L + 3L_N}(t - t_k) \tag{21}$$

$$i_\alpha(t) = i_\alpha(t_k) + \frac{e_{av0}(t_k) - s_{1\alpha}(t_k) V_C(t_k)}{L}(t - t_k) \tag{22}$$

$$i_\beta(t) = i_\beta(t_k) + \frac{e_{av\beta}(t_k) - s_{1\beta}(t_k) V_C(t_k)}{L}(t - t_k) \tag{23}$$

where $s_{10}(t_k)$, $s_{1\alpha}(t_k)$, $s_{1\beta}(t_k)$ represent the first vector being in duty during the considered interval $(t_k, t_k + d_1 T_s)$.

The solutions (20)-(22) illustrate the segment ab in Fig. 4. The actual currents within further intervals are illustrated in Fig. 4 by the segments bc, cd and de, respectively.

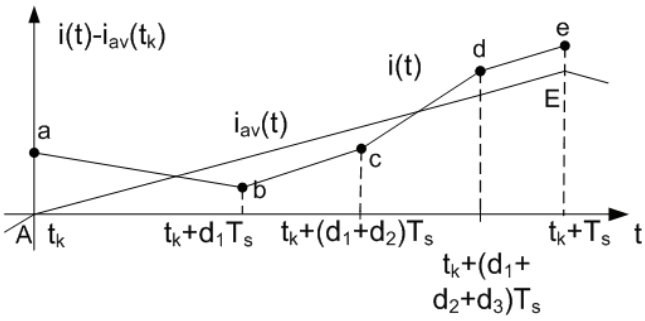

Fig. 4. Piecewise linear approximation of average and actual current within one switching period

The difference between actual currents and average currents is defined as ripple currents. For the first interval $(t_k, t_k + d_1 T_s)$ the ripple currents are

$$\Delta i_0(t) = i_0(t) - i_{av0}(t) = i_0(t_k) - i_{av0}(t_k) + \frac{(s_{10}(t_k) - e_{av0}(t_k)) V_C(t_k)}{L + 3L_N}(t - t_k) \tag{24}$$

$$\Delta i_\alpha(t) = i_\alpha(t) - i_{av\alpha}(t) = i_\alpha(t_k) - i_{av\alpha}(t_k) + \frac{(s_{1\alpha}(t_k) - e_{av\alpha}(t_k)) V_C(t_k)}{L}(t - t_k) \tag{25}$$

$$\Delta i_\beta(t) = i_\beta(t) - i_{av\beta}(t) = i_\beta(t_k) - i_{av\beta}(t_k) + \frac{(s_{1\beta}(t_k) - e_{av\beta}(t_k)) V_C(t_k)}{L}(t - t_k) \tag{26}$$

The ripple functions can be similarly expressed for the remaining intervals. It is easy to notice that ripple functions fulfil the condition

$$\int_{t_k}^{t_k + T_s} \Delta i(\tau) d\tau = 0 \tag{27}$$

Putting ripple functions (24)-(26) and similar equations written for remaining intervals into condition (27) the ripple magnitudes at instants t_k, $t_k + d_1 T_s$, $t_k + (d_1 + d_2) T_s$ and $t_k + (d_1 + d_2 + d_3) T_s$ can be computed. The analytical formulae for ripple magnitudes derived basing on the approximated waveforms shown in Fig. 4 are

$$\Delta i_{n0}(t_k) = \frac{V_C T_s}{2(L + 3L_N)}[(s_{n0} - s_{av0})(d_n^2 + 2d_n d_{n+1} + 2d_n d_{n+2} + 2d_n d_{n+3}) + (s_{(n+1)0} - s_{av0})(d_{n+1}^2 + 2d_{n+1} d_{n+2} + 2d_{n+1} d_{n+3}) + (s_{(n+2)0} - s_{av0})(d_{n+2}^2 + 2d_{n+2} d_{n+3}) + (s_{(n+3)0} - s_{av0}) d_{n+3}^2] \tag{28}$$

$$\Delta i_{n\alpha}(t_k) = \frac{V_C T_s}{2L}[(s_{n\alpha} - s_{av\alpha})(d_n^2 + 2d_n d_{n+1} + 2d_n d_{n+2} + 2d_n d_{n+3}) + (s_{(n+1)\alpha} - s_{av\alpha})(d_{n+1}^2 + 2d_{n+1} d_{n+2} + 2d_{n+1} d_{n+3}) + (s_{(n+2)\alpha} - s_{av\alpha})(d_{n+2}^2 + 2d_{n+2} d_{n+3}) + (s_{(n+3)\alpha} - s_{av\alpha}) d_{n+3}^2] \tag{29}$$

$$\Delta i_{n\beta}(t_k) = \frac{V_C T_s}{2L}[(s_{n\beta} - s_{av\beta})(d_n^2 + 2d_n d_{n+1} + 2d_n d_{n+2} + 2d_n d_{n+3}) + (s_{(n+1)\beta} - s_{av\beta})(d_{n+1}^2 + 2d_{n+1} d_{n+2} + 2d_{n+1} d_{n+3}) + (s_{(n+2)\beta} - s_{av\beta})(d_{n+2}^2 + 2d_{n+2} d_{n+3}) + (s_{(n+3)\beta} - s_{av\beta}) d_{n+3}^2] \tag{30}$$

where $n = 1,2,3,4$ means the number of subinterval within considered switching period, with $d_5 = d_1$, $d_6 = d_2$, $d_7 = d_3$, $s_5 = s_1$, $s_6 = s_2$, $s_7 = s_3$, $d_4 = 1 - (d_1 + d_2 + d_3)$ and $s_4 = 0$. For example, if $n = 1$ the ripple magnitude is computed at point ‘a’ (Fig. 4). For $n = 2,3,4$ the magnitudes at points ‘b’,’c’,’d’ are computed.

The ripple magnitudes of line currents can be computed from the ripple magnitudes of $0, \alpha, \beta$ components by linear transformation (3)

$$\begin{bmatrix} \Delta i_{na}(t_k) \\ \Delta i_{nb}(t_k) \\ \Delta i_{nc}(t_k) \end{bmatrix} = T^{-1} \begin{bmatrix} \Delta i_{n0}(t_k) \\ \Delta i_{n\alpha}(t_k) \\ \Delta i_{n\beta}(t_k) \end{bmatrix} \tag{31}$$

The formulae derived above enable one to compute the ripples for any specific realization of power active filter.

Example – third order harmonic generation in the three-phase four-leg circuit

Assume that third order harmonic should be generated in the circuit shown in Fig. 1. The results of computation have been obtained for the following circuit parameters: $e_a = 600\sin(314t)$ and source voltages are balanced, $L = 20$ mH, $L_N = 1$ mH, $R = 0.08\Omega$, $T_s = 0.1\mu s$, C=50 μF, $V_C(0) = 1000$ V.

The assumed currents to be generated are

$$i_a(t) = 20\sin(3 \cdot 314t) + 1.3\sin(314t)$$

$$i_b(t) = 20\sin(3 \cdot 314t) + 1.3\sin(314t - 2\pi/3)$$

$$i_c(t) = 20\sin(3 \cdot 314t) + 1.3\sin(314t + 2\pi/3)$$

The fundamental harmonic has to be added in order to ensure the energy balance. The assumed source voltages and current generated are shown in Fig. 5.

The ripple magnitudes of line currents at point ‘a’ (Fig. 4) computed with the use of the derived formulae (28)-(31) for $n = 1$ are shown in Fig. 6.

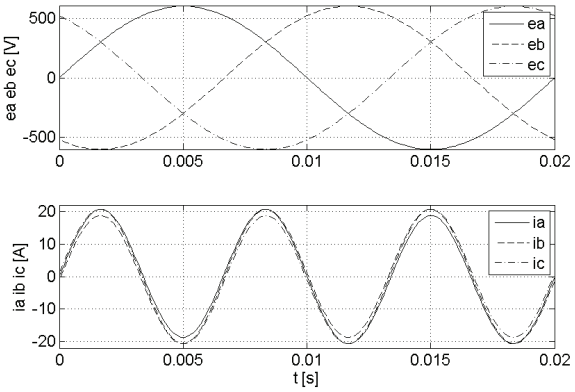

Fig. 5. Source voltage and generated current

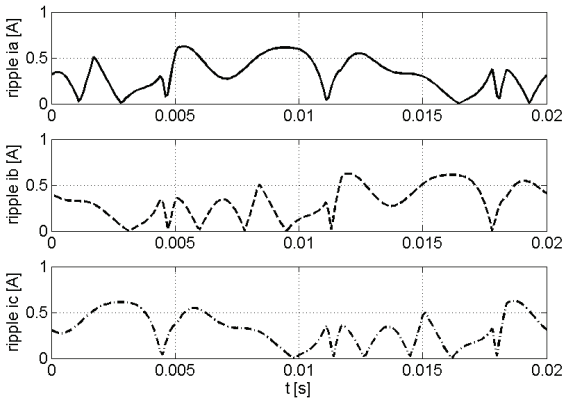

Fig. 6. Ripple absolute value of line currents within first duty ratio interval

By putting $n = 1,2,3,4$ in (28)-(31) the ripple magnitudes at points ‘a’, ‘b’, ‘c’, ’d’ (Fig. 4) can be computed. The results are shown in Fig. 7.

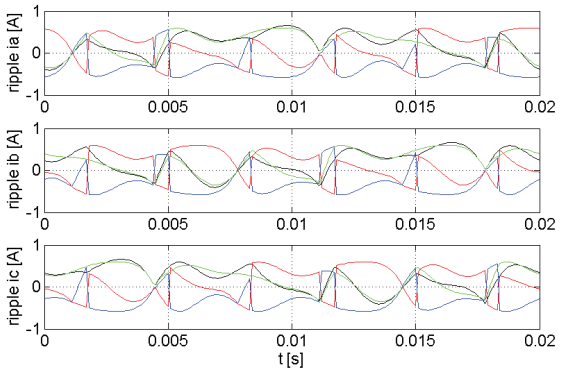

Fig. 7. Ripples of line currents within four duty ratio intervals

Conclusions

The current ripples can be computed by simulation of a specific PWM realisation. More general information can be obtained from analytical formulae. The average technique is a very convenient tool to analyze the behavior of ripples within the switching process. Especially such analysis is useful when the filter inductance and switching frequency is chosen.

REFERENCES

[1] X. Mao, R. Ayyanar and H. K. Krishnamurthy, Optimal Variable Switching Frequency Scheme for Reducing Switching Loss in Single – Phase Inverters Based on Time – Domain Ripple Analysis, IEEE Trans. Power Electron., vol. 24, No. 4, pp. 991-1001, 2009

[2] R. Zhang, H. Prasad, D. Boroyevich, and F. C. Lee, Averaging Three-Dimensional Space Vector Modulation for Four-Leg Voltage-Source Converters, IEEE Trans. Power Electron., vol. 17, No. 3, pp. 314-326, 2002

[3] K. Mikołajuk, A. Toboła, Ripple estimation in active power filters, Przegląd Elektrotechniczny, No. 5, 2011, pp.111-115

Authors: prof. Kazimierz Mikołajuk, e-mail: mik@iem.pw.edu.pl; mgr. Inż. Andrzej Toboła, Warsaw Technical Unversity